• U C •

FCTUC FACULDADE DE CIÊNCIAS
E TECNOLOGIA
UNIVERSIDADE DE COIMBRA

DEPARTAMENTO DE
ENGENHARIA MECÂNICA

Thermal Management of Photovoltaic Cells based on Constructal Law

Submitted in Partial Fulfillment of the Requirements for the Degree of Master in Mechanical Engineering in the specialty of Energy and Environment

Author

Miguel Rolinho Clemente

Supervisor

Professor Doutor Miguel Rosa Oliveira Panão

Jury

President	**Professor Doutor Adélio Manuel Rodrigues Gaspar** **Professor Auxiliar da Universidade de Coimbra**
Vowel	**Professor Doutor José Joaquim da Costa** **Professor Auxiliar da Universidade de Coimbra**
Supervisor	**Professor Doutor Miguel Rosa Oliveira Panão** **Professor Auxiliar da Universidade de Coimbra**

Institutional Collaboration

Associação para o Desenvolvimento da Aerodinâmica Industrial

Coimbra, September, 2015

"Nature never breaks her own laws."
Leonardo da Vinci

"The future belongs to those who believe in the beauty of their dreams."
Eleanor Roosevelt

Acknowledgments

To my parents, siblings and family, for the love, trust and moral support devoted in all my life.

To Diana, for the encouragement, patience and affection, vital to this journey.

To André, João and Mariana, for the companionship and assistance in our works.

To all my friends without who I wouldn't be here now, or would have got here faster.

To all the teachers and colleagues whom have incited me in the search of knowledge and wisdom.

To Prof. Dr. Miguel Panão for the help and guidance throughout this work.

Abstract

The increase of temperature on PV cells is considered one of the most critical issues that affects their efficiency, promoting degradation and cell life reduction. Therefore, thermal management is essential and must be an integral part of PV systems. In this thesis, the constructal law is explored as a design tool to develop a thermal management system for PV cells, based on single-phase forced convection.

In order to cool the PV cell rectangular area, a tree-network structure has been chosen to test the constructal theory approach. Considering this, an experimental facility has been built with 3D printing. The voltage and temperature output of a PV cell has been characterized with and without thermal management. The results evidence an improvement of 32 % on the PV cell efficiency through a decrease in the temperature coefficient ($\partial V/\partial T$) of 16.5 %. Therefore, constructal design applied to cooling technology shows great potential to improve photovoltaic thermal managements.

Keywords: Constructal, Photovoltaic, Cooling, 3D Printing

Resumo

O aumento da temperatura em células fotovoltaicas é considerado um dos problemas mais críticos que afeta a sua eficiência, promovendo degradação e redução da vida útil da célula. Portanto, o controlo da temperatura é essencial e deve ser uma parte integrante dos sistemas fotovoltaicos. Esta tese explora a lei construtal para desenvolver uma instalação experimental para arrefecimento das células fotovoltaicas.

De forma a arrefecer a área retangular da célula fotovoltaica, foi escolhida uma estrutura em árvore para testar a abordagem da teoria construtal. Tendo isto em consideração, foi construída uma instalação experimental com impressão 3D. A voltagem produzida e a temperatura da célula fotovoltaica foram caracterizados com e sem o sistema de gestão térmica. Os resultados evidenciam um melhoramento de 32 % na eficiência da célula através de uma redução no coeficiente de temperatura ($(\partial V/\partial T)$ de 16.5 %. Portanto, o design construtal aplicado a tecnologia de arrefecimento demonstra grande potencial para melhorar a gestão térmica de sistemas fotovoltaicos.

Palavras Chave: Construtal, Fotovoltaico, Arrefecimento, Impressão 3D

Contents

List of Figures

List of Tables

Nomenclature

A	Area	m^2
c_p	Specific heat	$J\,kg^{-1}K^{-1}$
D	Diameter	m
E_v	Illuminance	lx
F	View factor	
f	Friction factor	
g	Acceleration of gravity	$m\,s^{-2}$
Gr	Grashof number	
H	Height	m
h	Convection coefficient	$W\,m^{-2}K^{-1}$
I	Irradiance	$W\,m^{-2}$
k	Heat conductivity	$Wm^{-1}K^{-1}$
L	Length	m
L_c	Characteristic dimension	m
$\dot{m}$	Mass flow rate	$kg\,s^{-1}$
Nu	Nusselt number	

P	Perimeter	m
p	Pressure	Pa
Pr	Prandlt number	
q	Heat transfer rate	W
q''	Heat flux	$W\,m^{-2}$
Ra	Rayleigh number	
Re	Reynolds number	
T	Temperature	^{o}C
U	Velocity	$m\,s^{-1}$
V	Volume	m^3
W	Width	m

Greek Symbols

α	Absorptivity	
α_T	Diffusivity	$m^2\,s^{-1}$
β	Thermal Expansion Coefficient	K^{-1}
ϵ	Emissivity	
η	Luminous Efficacy	$lm\,W^{-1}$
μ	Dynamic Viscosity	$kg\,m^{-1}s^{-1}$
ν	Kinematic Viscosity	$m^2\,s^{-1}$
ϕ_v	Luminous Flux	lm
ρ	Volumic Mass or Density	$kg\,m^{-3}$

σ	Stefan-Boltzmann Constant	$5.670 \times 10^{-8}\, W\, m^{-2}\, K^{-4}$

Subscripts

a	air, ambient
b	back surface
cs	cooling system
f	front surface
fc	forced convection
inc	incident
nc	natural convection
rad	radiation

Acronyms

CTM	Constructal Thermal Management
PV	Photovoltaic

1 Introduction

1.1. Motivation

Solar energy is an important source of renewable energy, widely employed and with a broad range of applications, from which stands out, mostly, the production of domestic hot water from solar collectors and of electricity through photovoltaic cells. Photovoltaics, ordinarily abbreviated as PV, is a simple and elegant technology to harness the sun's energy. PV cells are unique devices, converting incident solar radiation into electricity without noise, pollution or moving parts. Built with semiconductors, which have the ability to transform energy available in solar radiation, either direct or diffuse, into electricity with a conversion efficiency, mainly determined by the semiconductor from which the cells are manufactured. PV technology has been adopted worldwide as solar energy is universal and abundant on the Earth's surface. Although PV systems have been commercialized and in use for many years, there are certain obstacles that mitigate a more disseminated utilization of this technology. Obstacles such as a limited conversion efficiency on the performance of PV cells, especially in solar wrenched hot climate areas, where cell temperature easily rises. The elevation of temperature on PV cells is considered as one of the most critical issues that affects their efficiency, promoting cell degradation and time life reduction. Therefore, thermal management is essential and should be an integral part of PV systems.

1.2. Temperature Effect on PV Cells

PV cells absorb up to 80% of the incident solar radiation, however only a small fraction of the absorbed incident energy is converted into electricity, depending on the efficiency conversion of the cell. The remaining energy is dissipated in the form of heat on the surface of the PV cell, which can reach temperatures up to $40\,^{\circ}C$ above the ambient temperature (Van Helden *et al.* , 2004). This happens because only a certain incident radiation wavelength is converted into electricity, due to the semiconductor

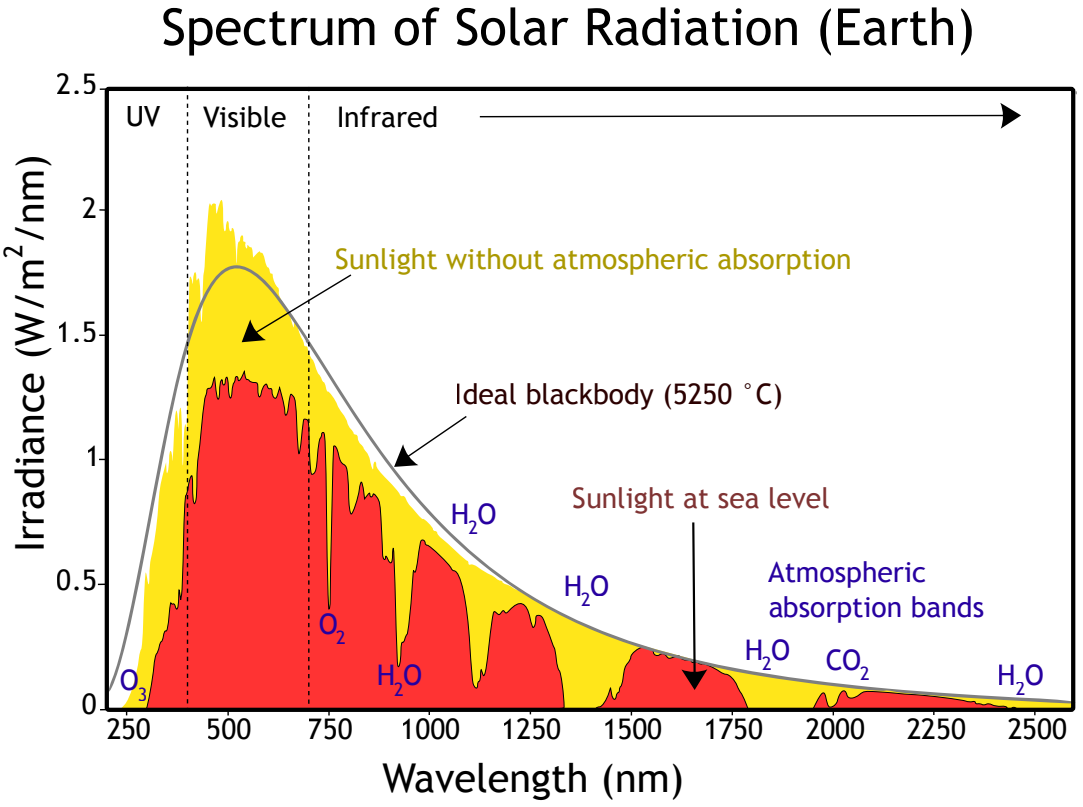

Figure 1.1: Solar Spectrum © Robert A. Rhode

band gap, while the rest dissipates itself as heat. The photoelectric conversion efficiency of crystalline Silicon PV cells commercially available is between 17 and 25% under optimum conditions, corresponding to standardized test conditions of AM 1.5 spectrum at $25\,°C$, where AM is the air mass coefficient that defines the direct optical path length through the Earth's atmosphere (Green *et al.* , 2010). However, PV cells do not work at optimum conditions, since temperature variations limit PV systems' efficiency. This drop in efficiency is related with the semiconductor band gap; for instance, Silicon band gap comprises wavelengths between $400\,nm$ and $1200\,nm$, comprising infrared and visible light radiation (Fig. 1.1). This means the remaining incident radiation is not energetic enough to excite the semiconductor electrons producing electricity. However, infrared radiation overexcites Silicon electrons, thus, is also not used to produce electricity. As temperature rises, the band gap decreases, causing less and less energy available to generate an electric current and increase the amount of radiation dissipating into heat (Mah, 1998; Luque & Hegedus, 2003).

Several factors damage the performance of PV cells in outdoor applications. Low

irradiance, high temperatures and soiling have a negative impact on the PV cell efficiency and lifespan. However, PV cells are mostly affected by high temperatures. In Silicon at $25\,^{\circ}C$, open circuit voltage declines at about $-2.3\,mV\ \cdot^{\circ} C^{-1}$.

1.3. Thermal Management of PV Cells

In order to prevent the effect of temperature on PV cells, the excess of heat must be removed. Therefore, thermal management systems should be an integral part of PV systems. Various methods can be employed to cool PV cells, however these can be grouped into two categories, passive and active cooling.

Passive cooling methods cover technologies that extract heat and/or minimize heat absorption from PV cells without consuming power. These methods imply heat transfer and dissipation to the environment. There are many options regarding passive cooling, some of them are simple like using high thermal conductivity fins, made of aluminum or copper (Cuce *et al.* , 2011). Or more complex methods, that use phase change materials (PCM) and several techniques of natural circulation of air (Biwole *et al.* , 2013). However, in passive cooling most of the heat transfer is performed by natural convection and radiation. These mechanisms are limited by the contact between the heat sink and the surrounding environment, conditioning the convective and radiative coefficients. Thus, these methods promote heat exchanges with a lower order of magnitude ($10^1 W/m^2$) compared to active cooling systems ($10^3 W/m^2$), which is particularly relevant in hot climate areas.

Active cooling systems consist of devices that move a fluid, gas or liquid, to extract heat through forced convection and conduction. Although these systems consume energy, called parasitic energy, they are normally applied in situations where the benefit to efficiency is larger than the necessary energy consumed. There are also cases where active cooling systems have an additional benefit, namely, recovering heat. By reusing the heated fluid as a heat source, it is possible to power, for example, a domestic hot water circuit (Odeh & Behnia, 2009; Moharram *et al.* , 2013).

In both cases, the most used mediums for heat transfer are air and water. However, air has thermal properties that make it less efficient as a cooling medium, therefore, in cases when there is a large accumulation of heat, air cooling is not the best solution because its use would require a greater consumption of parasitic energy than for the

same amount of heat removed by a water cooling system. Also, with air, heat recovery is more difficult and less efficient. However, in environments where water is scarce, air cooling is a viable option. Water cooling allows performing on a higher level of temperature differences and a much more efficient heat recovery. Many systems combine active and passive elements for an increased performance. The choice of cooling method and medium is strictly dependent on PV system operating conditions.

Finally, considering active thermal management systems, a question emerges on how are these systems designed. What is the best channel configuration that promotes heat exchanges and produces less resistance to the flow, decreasing pump losses and, consequently, allowing to decrease the consumption of parasitic energy? Recently, a new law, the Constructal Law, has been proposed by Adrian Bejan, Professor at Duke University, that explains how configurations evolve in time, and this is the approach followed in this work. The next section is dedicated to briefly review the Constructal Law.

1.4. Constructal Law

Through the Constructal Law, we understand that the physical phenomena associated with flow systems generation in nature can be rationalized in the evolution of the configuration of the currents that flow through it. In Bejan & Lorente (2008), the constructal law is defined as

> For a finite-size flow system to persist in time (to live), its configuration must change in time such that it provides easier and easier access to its currents (fluid, energy, species, etc.).

By perceiving that a flow configuration is free to morph in time, in order to improve the global flow of the system and that this principle is observable in all fields of nature, a new approach to the design of flow systems emerges, and with it, the possibility to predict, explain, and construct natural specific geometric characteristics (Bejan & Zane, 2012).

Constructal theory is about the optimization of an easier access of a flow from point A to point B, be them either a single point or an "infinity" of points (area or volume). It is fairly simple to give an example of a flow and show the constructal law in action.

Looking at the human respiratory system, where from a single intake of air, it flows to smaller and smaller components to be easily distributed to an infinity of smaller points, covering a larger area. And if we compare this human example to a tree, we can see the similarities, the sap flows from the roots of the tree to the leaves through the trunk and increasingly smaller branches. This tree shaped configuration is, theoretically, the easiest way to provide access from a single point to an "infinity" of points, and the easiest configuration to understand the universality of the constructal principle.

In constructal law, design is not an overlooked feature of a system, it is a scientific method that minimizes trial-and-error and increases a system's performance. One main aspect of the application of the constructal law is that imperfections cannot be eliminated, only reduced and distributed along the flow. In this way, their impact on the flow can be minimized. Imperfections can be quantified as entropy generators, an irreversibility that in a flow is determined by a pressure drop, or a temperature difference. Thus, the essence of the constructal law is to obtain an increasingly better design until the optimum distribution of imperfections is achieved, obtaining a configuration that is not perfect but is the least imperfect possible. This enlightens an important property of a flow geometry, *Svelteness*.

Svelteness characterizes the relation between the flow's external and internal scales and describes the relative importance of distributed losses along the flow, as well as the localized losses in junctions, curves, contractions and expansions. When calculating global pressure drop, it has been common to neglect local losses. Svelteness shows that this simplification is not always true. In this way, Svelteness is a design parameter that helps engineering by orientating the evaluation of the flow efficiency.

Finally, although the constructal law is universal, the configurations obtained from it are not. There is an infinite number of possible configurations to flow a fluid from one point to another. But if the purpose of design is to flow from one point to an "infinity" of points, the tree-shaped geometry is the best configuration, which is used in the example that follows, in order to understand the heat and fluid flow analysis underlying a constructal law approach.

The T-shaped construct is the simplest tree (Fig. 1.2), where the flow connects one point with two other points, and has two global constraints: i) total duct volume (Eq. 1.1); ii) and total space area (Eq. 1.2).

$$V = \frac{\pi}{4}(D_1^2\, L_1 + 2D_2^2\, L_2) \tag{1.1}$$

$$A = 2\, L_2\, L_1 \tag{1.2}$$

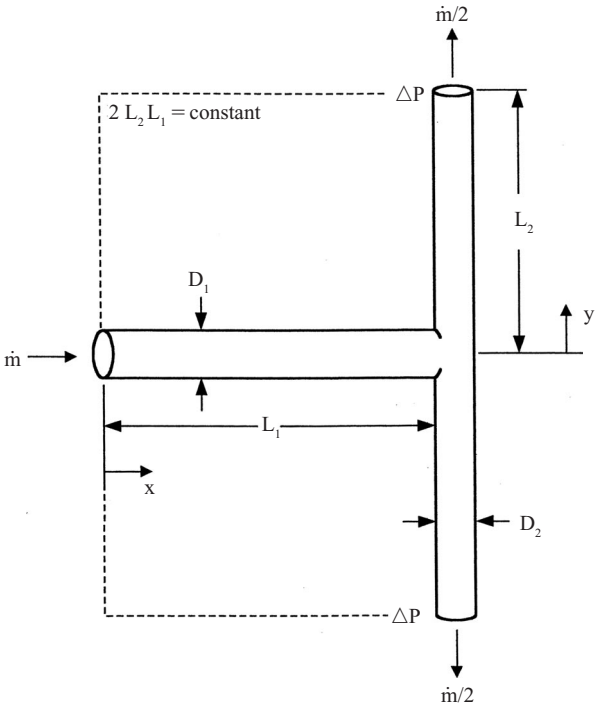

Figure 1.2: T-shaped construct of round tubes

Considering a laminar flow, and assuming negligible local pressure losses compared with distributed pressure losses, the pressure drop along each tube is deducted from the friction factor:

$$f = \frac{\frac{dp}{dx} D}{\frac{1}{2}\rho U^2} \tag{1.3}$$

which solved for the pressure difference and after discretization becomes

$$\Delta p = f\, \frac{1}{2}\rho\, U^2\, \frac{L}{D} \tag{1.4}$$

Considering round tubes and a Poiseuille flow, the friction factor is also correlated to the Reynolds Number as

$$f = \frac{64}{Re} \tag{1.5}$$

with the Reynolds Number, for round tubes (diameter D as length scale), defined by:

$$Re_D = \frac{\rho\, U\, D}{\mu} \tag{1.6}$$

Thus, considering the mass flow rate $\dot{m} = \rho A U$, where $A = \frac{\pi}{4} D^2$ is the area, and $\nu = \mu/\rho$:

$$\Delta p = \frac{128\, \nu\, \dot{m}\, L}{\pi\, D^4} \tag{1.7}$$

This relation is applied to each tube, thus, becoming

$$\Delta p_1 = \frac{128\, \nu\, \dot{m}_1\, L_1}{\pi\, D_1^4} \tag{1.8}$$

$$\Delta p_2 = \frac{128\, \nu\, \dot{m}_2\, L_2}{\pi\, D_2^4} \tag{1.9}$$

Since the T-shape is symmetric, $\dot{m}_1 = 2\dot{m}_2$, thus, the global pressure drop is $\Delta p = \Delta p_1 + \Delta p_2$, and given by

$$\Delta p = \frac{128\, \nu\, \dot{m}_1}{\pi} R_{lam} \tag{1.10}$$

where R_{lam} is the simplification of the pressure drop sum and represents a factor dependent on the T geometry as

$$R_{lam} = \frac{L_1}{D_1^4} + \frac{L_2}{2\, D_2^4} \tag{1.11}$$

To minimize the total pressure drop, R_{lam} must be optimized. Increasing D_1 and D_2 is not the solution, since they are associated with a volume constraint. To optimize D_1 and D_2 is equivalent to minimize R_{lam} while keeping V constant. We achieve this with the method of Lagrange Multipliers:

$$\Phi = \frac{L_1}{D_1^4} + \frac{L_2}{2\, D_2^4} + \lambda\, (D_1^2\, L_1 + 2 D_2^2\, L_2) \tag{1.12}$$

which is a combination of R_{lam} and V. The Lagrange multiplier is λ. By solving the following system of equations, the extremum of Φ is found:

$$\frac{\partial \Phi}{\partial D_1} = \frac{-4\, L_1}{D_1^5} + \lambda\, 2\, D_1\, L_1 = 0 \tag{1.13}$$

$$\frac{\partial \Phi}{\partial D_1} = \frac{-2\, L_2}{D_2^5} + \lambda\, 4\, D_2\, L_2 = 0 \tag{1.14}$$

and we discover that L_1 and L_2 do not influence the diameter ratio, and by eliminating the Lagrange multiplier we obtain:

$$\frac{D_1}{D_2} = 2^{1/3} \tag{1.15}$$

which is known as the Hess-Murray rule, independent on the length and geometry of the tubes. This rule is applicable on perfect symmetric bifurcations, because if the bifurcation is asymmetrical the diameters ratio will depend on their lengths.

Further optimization of the geometry in order to minimize total pressure drop is related to the construction features and design focuses. In section 2.3.2, this issue is explained in more detail, and aimed at the objectives of this work.

1.5. Objectives

This dissertation aims to design and develop an experimental setup of a thermal management system to cool a PV cell based on the Constructal Law. The correlation between the voltage produced by the PV cell and its temperature is investigated, as well as the effect of a Constructal Thermal Management (CTM) on the PV cell efficiency.

2 Experimental Facility

2.1. Facility Structure

This dissertation has the objective of developing an experimental facility to study thermal management of PV cells. The facility consists of a support structure, a source of irradiance and the PV cell with or without the thermal management system.

2.1.1. Support Structure

The facility requires a support structure to perform a proper adjustment of the PV cell position, so that the level of energy incident on the cell surface can be adjusted as required. A working bench is used with a ruled rail ($1000\,mm$), where a bracket can be mounted that allows a millimetric control of the position of the PV cell (Fig. 2.1).

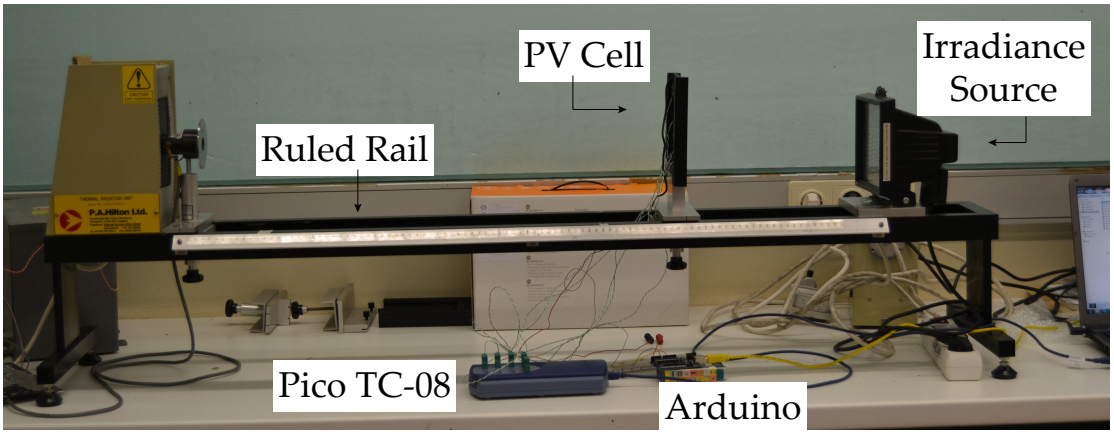

Figure 2.1: Support Structure

2.1.2. Irradiance Source

The irradiance source is mounted in one of the extremities of the support structure, $80\,mm$ from the $1000\,mm$ ruled rail. It simulates sunlight exposure to the PV cell, using a projector for RS7 - 118 mm lamps, which is equipped with a $400\,W$ Halogen

OSRAM HALOLINE® ECO SUPERSTAR lamp (Fig. 2.2). The projector is connected to an electrical outlet with a switch to manually switch it on and off.

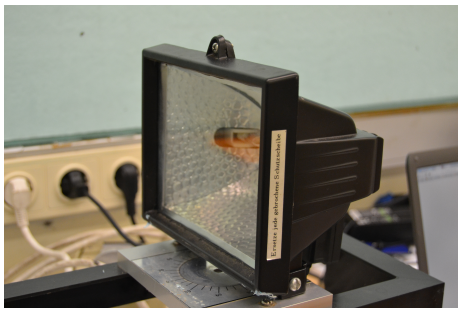

Figure 2.2: Irradiance Source

2.2. PV Cell and Support

2.2.1. PV Cell

The PV cell used in this experimental setup is a $2\,W$ Solar Panel from Voltaic Systems (Fig. 2.3). It is waterproof, scratch and UV resistant, as well as a compact and lightweight panel, with $135 \times 112 \times 5\,mm$ and $105\,g$. The panel output, from the manufacturer, under an irradiance of $1000\,W\,m^{-2}$, AM 1.5 and at $25\,°C$ is as follows:

- Monocrystalline Cell: 19% efficiency
- Open Circuit Voltage: $7.0\,V$
- Peak Voltage: $6.0\,V$
- Peak Current: $378\,mA$
- Peak Power: $2.27\,W$

2.2.2. PV Cell Support

A support to mount the PV cell on the bracket has been designed to avoid causing interference to light exposure and allow an easy replacement of the cell. This support would also be relevant to mount the thermal management system. Furthermore, the material required for the support should provide a good thermal insulation. Resorting to fast prototyping, the support has been 3D printed, with PLA, a light polymer with

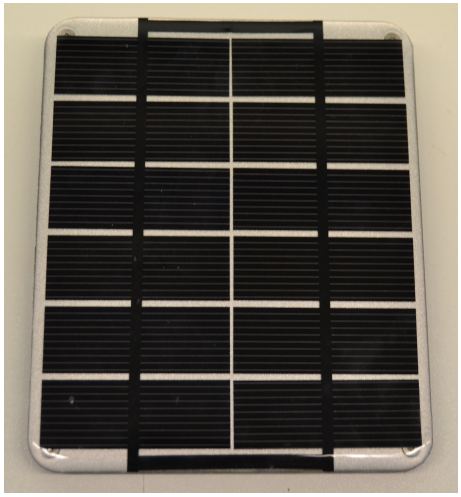

Figure 2.3: PV Cell

a thermal conductivity of $k = 0.13\,W\,m^{-1}K^{-1}$. Fig. 2.4 depicts the PV cell support (black) mounted on the bracket (silver).

Figure 2.4: PV Cell Support

2.3. Constructal Thermal Management System

The thermal management system is based on a high performance water cooling kit used for CPU cooling, an EK Water Blocks EK-KIT L120, from which we use the DC Pump with Reservoir and Radiator plus Fan. The pump is connected to the radiator

with a coupled fan, and through it, to the cooling interface (Fig. 2.5). Both DC Pump and Fan operate at $12\,V$ powered by a computer power supply. The design of the cooling interface based on the constructal theory is further detailed in Section 2.3.2.

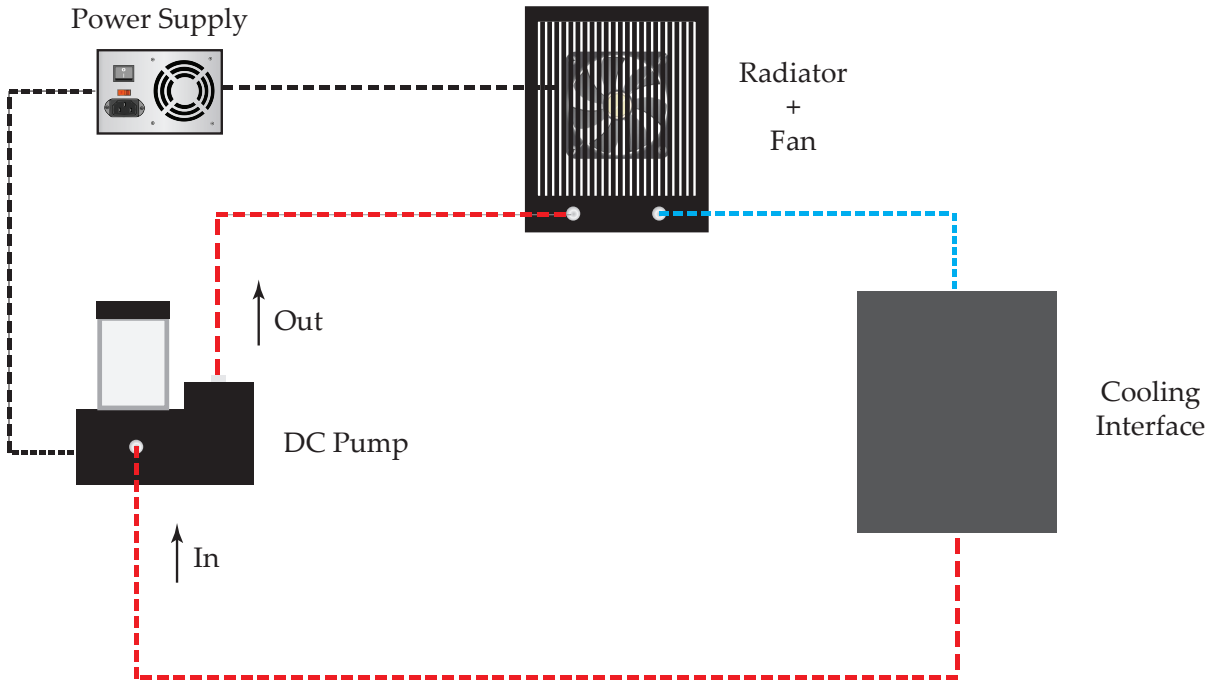

Figure 2.5: Scheme of the Thermal Management System

2.3.1. Thermal Analysis

In order to design the flow system, first we need to do a thermal balance on the PV cell. The PV cell front surface is irradiated by the light source and loses heat by convection to the ambient air, and by radiation to the environment. The back surface is to be maintained at a desired temperature, in this case of $25\,°C$, using the thermal management system.

From Fig. 2.6 we have q''_{inc}, the solar irradiated heat incident on the PV cell front surface, q''_{nc} is the heat lost by natural convection on the front surface, q''_{rad} is the heat lost by radiation to the environment from the front surface , and finnaly q''_{fc} is the heat transferred by forced convection from the back surface to the cooling system that should maintain the PV cell at $25\,°C$. At steady-state, the thermal balance is described by

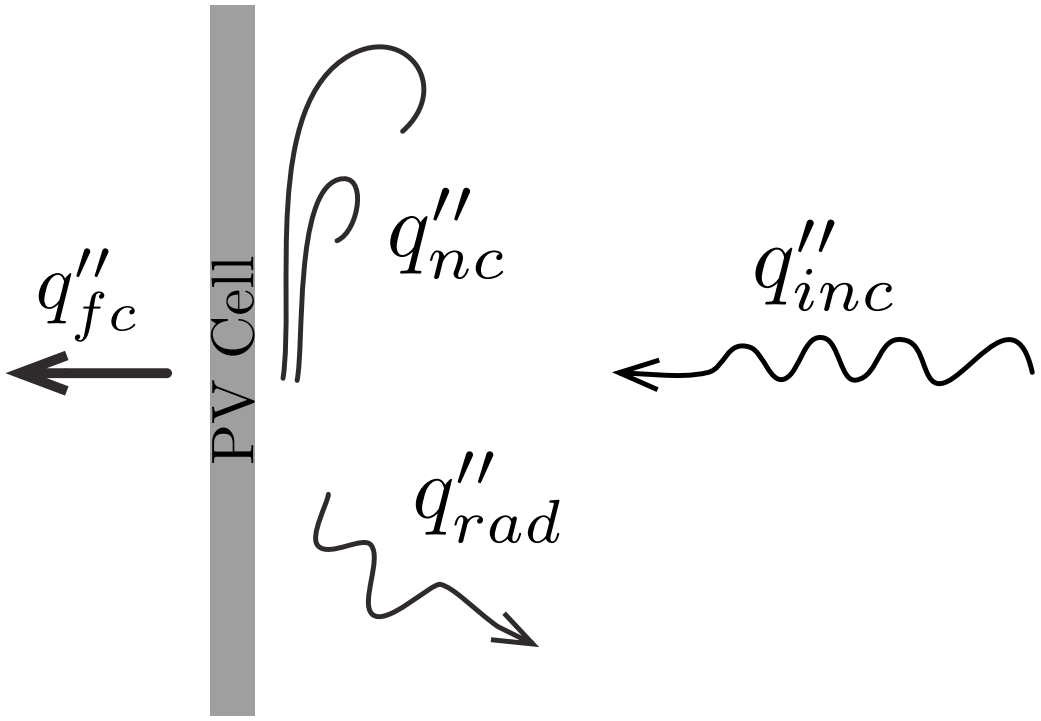

Figure 2.6: Scheme of Thermal Balance on PV Cell

$$0 = \alpha q''_{inc} - q''_{nc} - q''_{rad} - q''_{fc} \tag{2.1}$$

considering there is no internal generation of energy. From here we can find how much heat must be removed by the cooling system in order to maintain the PV cell at the desired operating temperature.

Regarding the PV cell properties, we consider only the effective dimensions of the cell, the length and height of the cell that comprise the semiconductor area, responsible for electricity generation. From Armstrong & Hurley (2010), the front surface emissivity is established as 0.91, these properties are listed in Table 2.1. In Table 2.2 are listed the properties of air at $20\,°C$ required for assessing the heat exchanges by convection and radiation.

Length, L	$124\,mm$
Width, W	$100\,mm$
Emissivity, ϵ	0.91

Table 2.1: PV Cell Properties

T_a	$20\,^{\circ}C$
ρ_a	$1.101\,kg\,m^{-3}$
μ_a	$19 \times 10^{-6}\,kg\,m^{-1}\,s^{-1}$
k_a	$0.027\,W\,m^{-1}\,K^{-1}$
c_{p_a}	$1000\,J\,kg^{-1}\,K^{-1}$
α_{T_a}	$24.5 \times 10^{-6}\,m^2\,s^{-1}$
Pr_a	0.704
β_a	$0.0034\,K^{-1}$
ν_a	$17.26 \times 10^{-6}\,m^2\,s^{-1}$

Table 2.2: Air Properties at 20°C

Radiation

Considering a solar irradiance of $I_S = 1000 W m^{-2}$, from Kirchoff Law, the absorptivity (α) is considered equal to emissivity (ϵ) for black and grey bodies, and to real surfaces when the temperature difference is lower than 50 - $80\,^{\circ}C$, which is the case (see later in sub-section 3.2.2).

Relatively to the net radiative balance,

$$q''_{rad} = J - G$$

where J is the radiosity and G the irradiance from the surroundings. Since the radiosity corresponds to the energy emitted by radiation due to the surface temperature, $E = \varepsilon\sigma T^4$, plus the energy reflected from that irradiated, ρG,

$$q''_{rad} = E + \rho G - G = E - (1-\rho)G = E - \alpha G$$

Finally, since $\alpha = \varepsilon$, and $G = \sigma T_a^4$, the net radiative heat flux on the front surface is given by

$$q''_{rad} = \varepsilon\sigma(T^4 - T_a^4)F \tag{2.2}$$

where ε is the emissivity of the surface, $\sigma = 5.67 \times 10^{-8}$ is the Stefan-Boltzmann constant, T_a the environment temperature and F the view factor.

In a scenario close to a real case, we take into consideration two view factors, one for the involving air (sky) and one for the nearby ground, F_{fs} and F_{fg}, respectively

(Armstrong & Hurley, 2010). With $F_{fs} = \frac{1}{2}(1 + cos\beta_{fs})$ and $F_{fg} = \frac{1}{2}(1 - cos\beta_{fg})$. Then the heat loss by radiation becomes $q_{rad} = \varepsilon\sigma A(T^4 - T_a^4)(F_{fs} + F_{fg})$. However we take that sky and ground temperatures are alike and equal to ambient air. Thus making heat loss by radiation equal to Eq. (2.2).

King *et al.* (2004) use an equation that simplifies the thermal resistance of the PV cell and helps to predict the front surface temperature using the measured back surface temperature:

$$T_f = T_b + \frac{I_S}{1000}\Delta T \tag{2.3}$$

where ΔT is given, by empirical data, as $3\,^{\circ}C$ for PV cells with a constitution of glass/cell/polymer sheet and in a situation of open rack. The heat flux of incident radiation has been measured to be $I_S = 1000W/m^2$, thus solving Eq. (2.3) to find T_f considering the operating temperature of $T_b = 25°C$, and Eq. (2.2).

Natural Convection

The heat lost by natural convection depends on the temperature difference between the front surface and the ambient air and the convection coefficient, h.

$$q''_{nc} = h_a(T_f - T_a) \tag{2.4}$$

$$h_a = Nu_a \times \frac{k_a}{L} \tag{2.5}$$

where Nu is the Nusselt number, representing relation between the thermal resistance of pure conduction on the thermal boundary layer in the panel, and the thermal resistance associated with convective heat transfer. In order to verify the boundary layer regime, the Rayleigh number which is the relation between buoyancy and viscosity within a fluid

$$Ra_L = \frac{g\beta(T_f - T_a)L^3}{\nu_a\alpha_{T_a}}$$

where L is the PV cell height, β the volumetric expansion thermal coefficient (assuming the air as an ideal gas, $\beta = 1/T_a$ with T_a in Kelvin), g the acceleration of gravity, ν_a and α_{T_a} the air's kinematic viscosity and thermal diffusivity, respectively. For the operation conditions considered, $Ra_a = 753.83$, thus it is in the laminar regime as

expected. For a vertical plate, the empirical correlation valid for the laminar regime with better accuracy is given by Churchill & Chu (1975) as

$$Nu_a = 0.68 + \frac{0.67Ra_L^{1/4}}{(1+(\frac{0.492}{Pr_a})^{9/16})^{4/9}} \tag{2.6}$$

The Prandtl Number, $Pr = \nu/\alpha_T$, in the correlation describes the ratio between molecular diffusivity of momentum and heat molecular diffusibility, associated with the relative thicknesses of the thermal and velocity boundary layers.

The result of Eqs. (2.4), (2.5) and (2.6), is the heat loss by natural convection.

Forced Convection

With the knowledge of three of the heat fluxes involved in the PV cell thermal balance, the heat transferred by force convection required to maintain the back surface at $25\,^{\circ}C$ is determined by Eq.2.1. The resulting value is given by

$$q''_{fc} = \alpha q''_{inc} - q''_{nc} - q''_{rad}$$

Now that we know how much heat should be removed by the cooling system we can analyze the flow movement and heat transfer through flow design. In the following section, the flow characteristics for the design are calculated.

2.3.2. Constructal Design

Geometry

The optimized tree structure is constrained with three geometric features: the smallest diameter (D_0), the total space area (A) and the tree-network complexity (n).

In section 1.4, the Hess-Murray rule (Eq. 1.15) regarding a single bifurcation has been deducted. However, in a tree-network, instead of a single bifurcation, we have a construct with a complexity n, where each increase of n means that each single tube bifurcates in two identical tubes, similar to Fig. 2.7, so that

$$\frac{D_{i+1}}{D_i} = 2^{1/3} \implies D_{i+1} = 2^{i/3}\, D_i \tag{2.7}$$

Since we intend to constrain the construct with the smallest diameter, the diameter of each construct level j, as a function of D_0, is

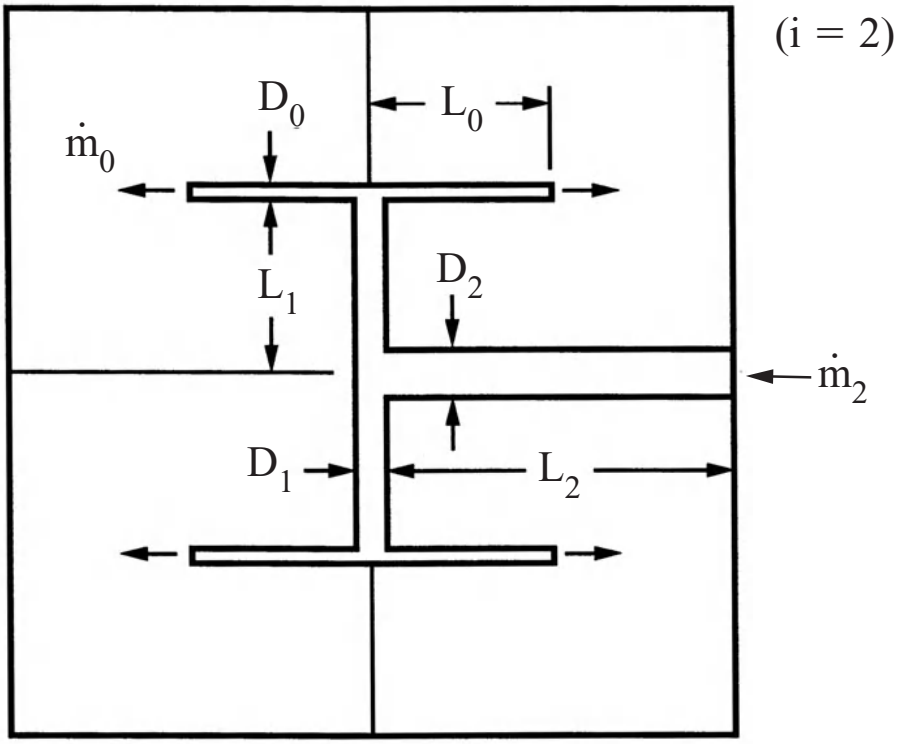

Figure 2.7: Scheme of a Constructal T-shaped Tree with $n = 2$

$$D_j = 2^{n-j/3}\, D_0 \tag{2.8}$$

where j varies from 0 to n and $j = n$ corresponds to $i = 0$.

Also, one of the construct features is that rectangular channels are used instead of round tubes, with W as width and H as height, thus, the hydraulic diameter is considered

$$D_h = \frac{4\,A}{P} = \frac{4\,H\,W}{2H + 2W} \tag{2.9}$$

We impose the smallest hydraulic diameter of $D_0 = 5/3\,mm$ and consider the depth H constant in all channels, $H = 3\,mm$. This means that for each tube we have to calculate the corresponding width W:

$$W_j = \frac{H\,D_j}{2H - D_j} \tag{2.10}$$

Following this, we need to determine the length L of all channels. From the dendritic

structure (Fig. 2.7) we can see that after the first bifurcation the length of channels is reduced only when the direction is repeated, $L_0 = L_1$ and $L_1 = L_2/2$.

To achieve this feature in the script, an orientation function is implemented

$$O(i) = 2^{mod(i,2)} \tag{2.11}$$

from which the orientation of the channel is represented by 1 and 2, horizontal and vertical respectively. Operation $mod(i, 2)$, known as modulo operation, is a computational operator that retrieves the remainder after division of i by 2.

We have imposed the smallest diameter (D_0), now by establishing the smallest length (L_0), we determine the elemental dimensions of the construct, from which the design is based. Thus, the smallest length is given by:

$$L_0 = \frac{0.5\sqrt{A}}{\prod O(i)} \tag{2.12}$$

where $\prod O(i)$ represents the effect of the complexity (n). Afterwards, the length of each channel is calculated as

$$L(j) = L_0 \prod_{j=0}^{n} O(n - j + 1) \tag{2.13}$$

Now that the dimensions of every channel are known, we can draw the constructal design. By using the constrains given in Tab. 2.3, a MATLAB® script has been made to generate the following dimensions (Tab. 2.4) and geometry (Fig. 2.8).

A	$124 \times 100\, mm^2$
D_0	$1\, mm$
n	6

Table 2.3: Constructal Constrains

Fluid Flow

After determining the geometry of the tree-network for performing thermal management of the PV cell, the fluid flow characteristics are analyzed. The assumptions of Sec. 1.4 are kept in the analysis, i.e. that the flow is in the Poiseuille regime and local

n	$W\,(mm)$	$L\,(mm)$
0	1.000	6.960
1	1.329	6.960
2	1.799	13.920
3	2.500	13.920
4	3.620	27.839
5	5.619	27.839
6	10.000	55.678

Table 2.4: Constructal Dimensions

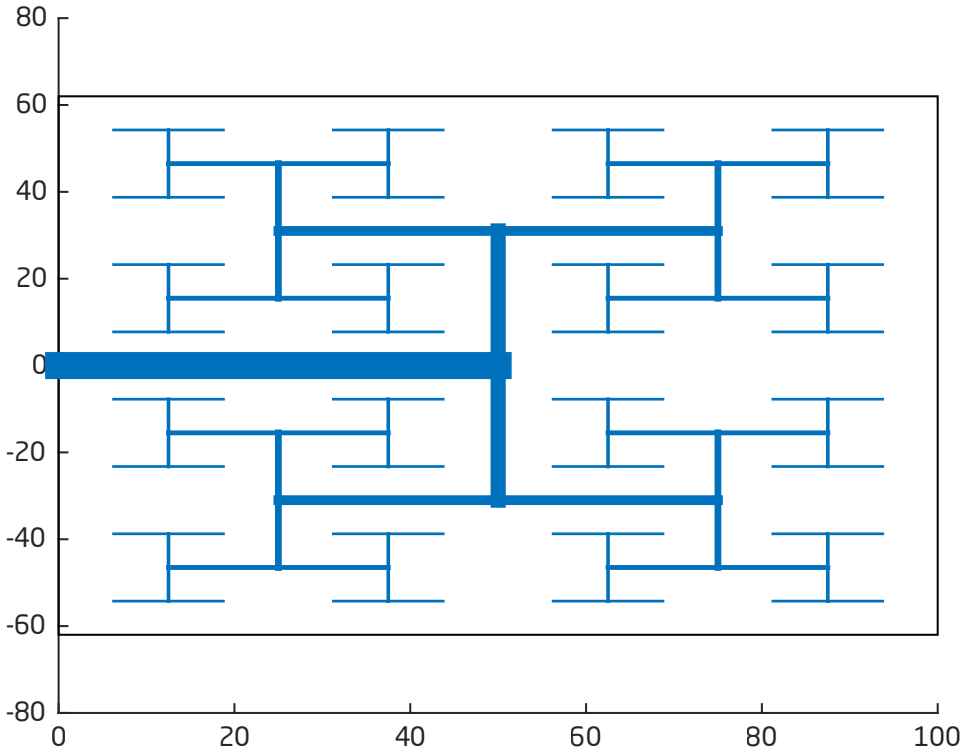

Figure 2.8: Scheme of the Constructal Design

pressure losses are neglected. If we consider Eq. (1.7), that is applied to each channel, the global pressure difference is the sum of pressure drop in all channels:

$$\Delta p = \sum_{i=0}^{n} \Delta p_i \tag{2.14}$$

Since we are using the Hess-Murray rule, global pressure difference is:

$$\Delta P = \frac{128\,\nu_w\,\dot{m}_0\,S_1}{\pi\,(D_0 \times 10^{-3})^4} \tag{2.15}$$

where S_1 is a sum that represents the effect of the complexity (n)

$$S_1 = \frac{2^{\frac{n+1}{6}} - 1}{2^{\frac{1}{6}} - 1} \tag{2.16}$$

The estimated pumping required to feed the flow is:

$$W = \frac{2^n\,\dot{m}_0\,\Delta P}{\rho_w} \tag{2.17}$$

And the flow regime with this configuration is:

$$Re = \frac{4\,\dot{m}_0}{\pi\,D_0\,\mu_w} \tag{2.18}$$

The flow system consists of two tree-network canopies, such as depicted in Fig.(2.8). The first serves as cooling interface, while the second collects the flow exiting the first tree. Between the cooling interface and the PV cell a Pyrolytic Graphite Sheet from Panasonic is placed, allowing a uniformization of the PV cell temperature distribution given its very high thermal conductivity ($> 1000\ W \cdot m^{-1}K^{-1}$), maximizing the heat transferred between the PV cell and the cooling system.

Heat Transfer

Considering a constant heat flow on the surface of the channels, as the one calculated in Sec. 2.3.1, the global heat transfer rate is given by $q = q''_{fc}\,A_b$, while the heat flux removed by the cooling system is $q''_{cs} = q\,\sum_{i=0}^{n}(W_i\,L_i)$ thus,

$$q''_{cs} = q''_{fc}\frac{A_b}{\sum_{i=0}^{n}(W_i\,L_i)} \tag{2.19}$$

where $W_i\,L_i$ is the surface of the channel in contact with the PV cell.

3 Methodology

3.1. Measurement Techniques

In this work, the correlation between the PV cell performance in terms of voltage supply and its temperature is made for several distances from the irradiation source. Thus, PV cell voltage and temperature are the two fundamental parameters that need to be measured. The measurement of voltage produced by the PV cell is performed using an Arduino UNO, a microcontroller board. Using a circuit that connects the PV cell to the Arduino we can read the input data and easily produce an output. The Arduino pins operate at $5\,V$, thus, in order to protect the microcontroller board, a circuit is devised to incorporate a series resistor (Fig. 3.1 [left]) and, in this way, the Arduino reads half the voltage produced by the PV cell. Since the maximum output is around $6\,V$, the damage of the microcontroller by the PV cell is avoided. The scheme in Fig. 3.1 (right) shows the positive pole connected to the analog pin A0. The board maps input voltages from 0 to $5\,V$ into integer values from 0 to 1023. This means the microcontroller has a resolution of $4.883\,mV/unit$. It takes about $100\,\mu s$ to read the analog input. The Arduino is connected via USB to a computer, this connection powers the microcontroller and serves as data acquisition. The data acquisition from the board is programmed and processed using the MATLAB® platform. The script is configured to acquire data at a sampling frequency of $1\,Hz$, which is much larger than the frequency associated with the timescale of temperature variations.

The temperature variation of the PV cell is measured in 5 locations (corners and center, as illustrated in Fig 3.2) using K type thermocouples, as well as the temperature at the inlet and outlet of the water flow used for cooling the cell.

The thermocouple signals where acquired with a Pico® TC-08 board and processed with PicoLog® software. The temperature acquisition rate has been also set to $1\,Hz$.

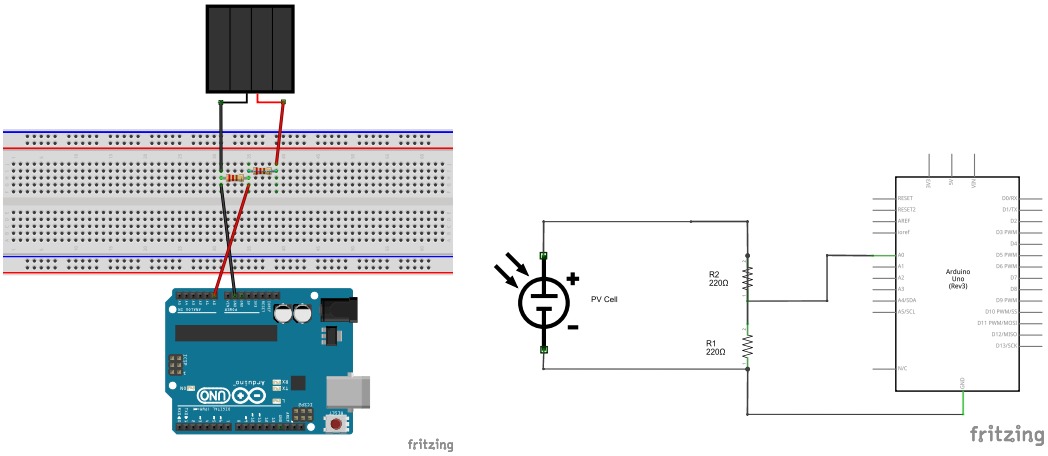

Figure 3.1: Representation of the circuit connecting the PV Cell to Arduino Uno (left) and Scheme of the circuit connecting the PV Cell to Arduino Uno (right)

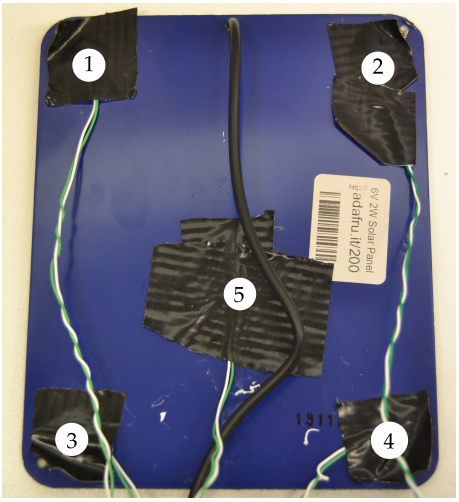

Figure 3.2: Position of Thermocouples in the Back of the PV Cell

3.2. Experimental Methodology

3.2.1. Irradiance Calibration

The irradiance I, or radiant flux received by a surface per unit area, is provided by a $400\,W$ Halogen OSRAM HALOLINE® ECO SUPERSTAR lamp, but it is important to measure the flux reaching the PV cell and perform a calibration with the distance between the PV cell and the light source. By measuring the illuminance E_v, in lux (lx), it is possible to correlate it with the irradiance $I\,[W\,m^{-2}]$, and calibrate the effective flux irradiated on the PV cell.

The illuminance E_v is equal to the ratio between the luminous flux ϕ_v in lumens

(lm) and the surface area $A\,[m^2]$:

$$E_v = \frac{\phi_v}{A} \tag{3.1}$$

Since luminous efficacy η is a relation between illuminance (E_v) and irradiance (I)

$$\eta = \frac{E_v}{I} \tag{3.2}$$

it is possible to measure the irradiance using the values of illuminace E_v provided by an OMEGA® HHF81 Light Meter. Additionally, the luminous efficacy is the relation between the lumens of a lamp and its corresponding power, if (3.1) is replaced in Eq. (3.2). Thus the halogen lamp used produces $8750\,lm$ and consumes $400\,W$, resulting in $\eta = 8750/400 = 21.875\,lm\,W^{-1}$.

By mounting the device in a support rail, the illuminance is measured every $50\,mm$ from $x_o = 335\,mm$ until the maximum illuminance reading supported by the device, which is at the $x = 1030\,mm$.

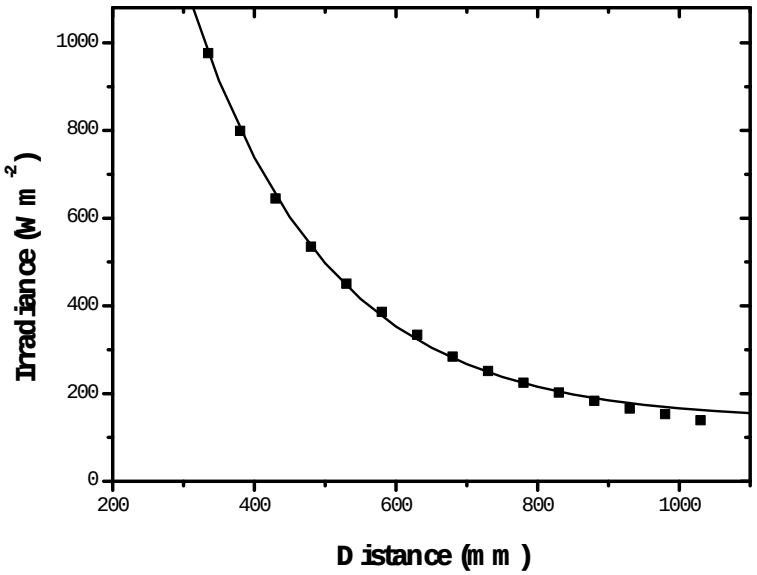

Figure 3.3: Calibration curve of irradiance as a function of distance from the light source.

By doing a non-linear regression based on an exponential function, the calibration of irradiance (I) as a function of position (x) from the light source to the PV cell, with a coefficient of correlation of $R^2 = 0.9996$, is devised as

$$I(x) = 138.971 + 837e^{-\frac{x-335}{194.327}} \tag{3.3}$$

3.2.2. PV Cell Characterization

Although the purpose is to design a thermal management system to keep the PV cell at a desired temperature, first it is important to characterize the response of the PV cell to temperature variation. In an initial phase, a PV cell is submitted to $I_S = 1000\,W\,m^{-2}$. In order to improve the heat transfer between the PV cell and the thermocouple, minimizing contact resistances, a thermal grease has been used (Titan Nano Grease) with a heat conductivity of $k > 4.5\,W\,m^{-1}K^{-1}$.

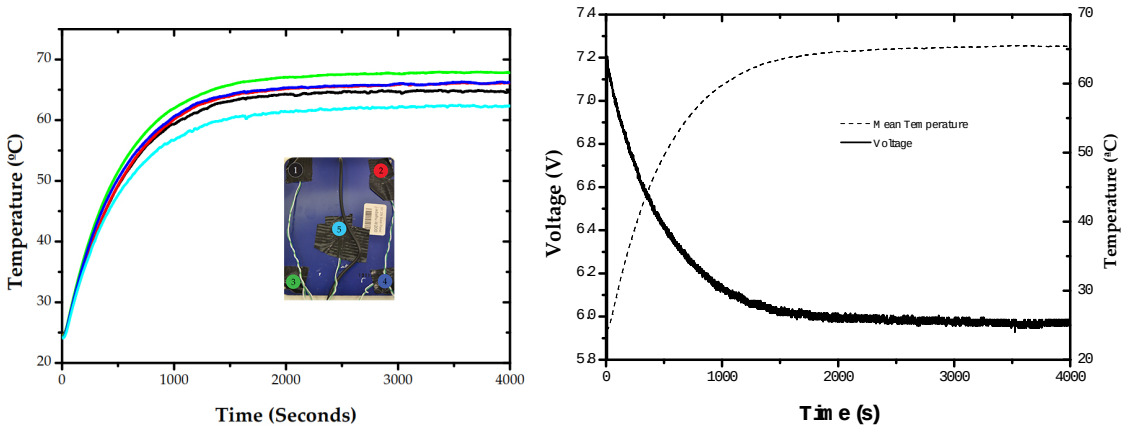

Figure 3.4: Temperature measurement in 5 location on the backside of the PV Cell (left) and evolution of both voltage and average temperature for $I = 1000\,W\,m^{-2}$ (right)

This test allows a first analysis on the response of the PV cell, and helps defining the proper total acquisition time, as well as allows to have some sensibility on the temperature distribution on the PV cell, in order to make a preliminary assessment of the uniformity degree. On the left hand side of Fig. 3.4, we can observe that thermocouples located in corners have similar temperature profiles, while at the PV cell center the stabilised temperature is about $6\,°C$ lower, indicating a non-uniform temperature distribution on the panel when the only cooling is by natural convection. If we now consider the average temperature between thermocouples and compare its evolution with the voltage provided by the panel (Fig. 3.4, on the right), the correlation between parameters is clear.

4 Analysis and Discussion of Results

In subsection 3.2.2 the response of the PV cell to irradiance has been characterized, and a clear correlation between temperature and voltage has been presented. With the installation of the Constructal Thermal Management (CTM) system, the response of the PV cell is expected to improve. In Fig. 4.1, the response of the system is depicted (PV cell voltage output and average temperature and water average temperature), and we can see a significant improvement, under the same irradiance, relatively to the use of the PV cell without a cooling system.

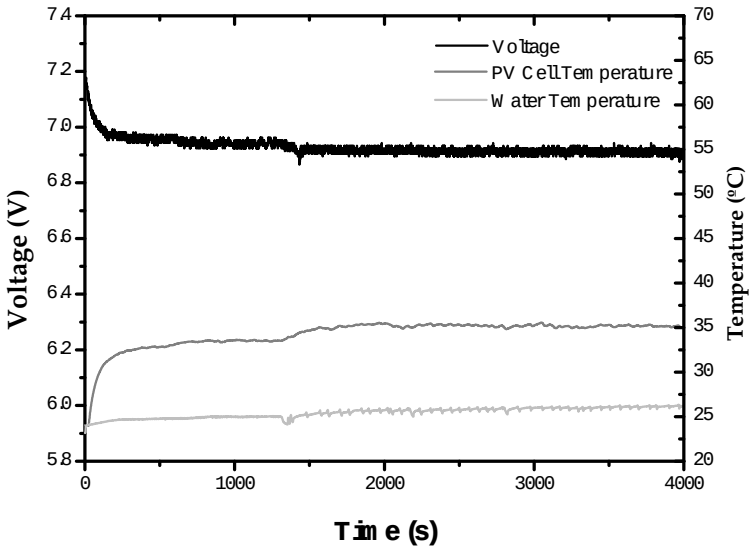

Figure 4.1: CTM System Response

Without CTM, at $I_S = 1000\,W\,m^{-2}$, the voltage drop is $\Delta V = 1.28\,V$, and the temperature difference is $\Delta T = 39.53\,°C$. If the CTM system is applied, voltage drop becomes $\Delta V = 0.31\,V$ and temperature increase $\Delta T = 11.56\,°C$. Fig. 4.2 compares voltage and temperature curves, and shows the differences between situations. We can also see the time it takes each system to stabilize an maintain their conditions, which is approximately the same.

By comparing the evolution of voltage - temperature evolution in each case, the effect the CTM exerts on the PV cell is clearer (Fig. 4.3). The slope corresponds

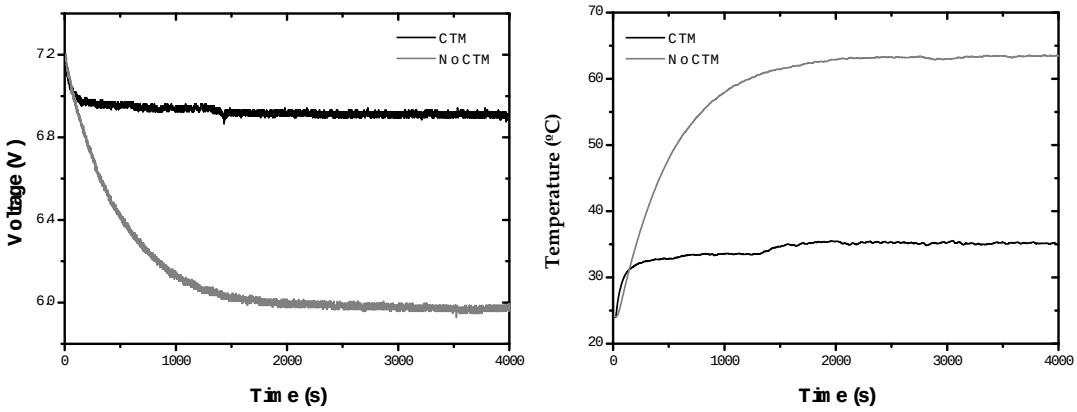

Figure 4.2: Evolution of Voltage (left) and Average Temperature of PV Cell (rigth) with and without CTM.

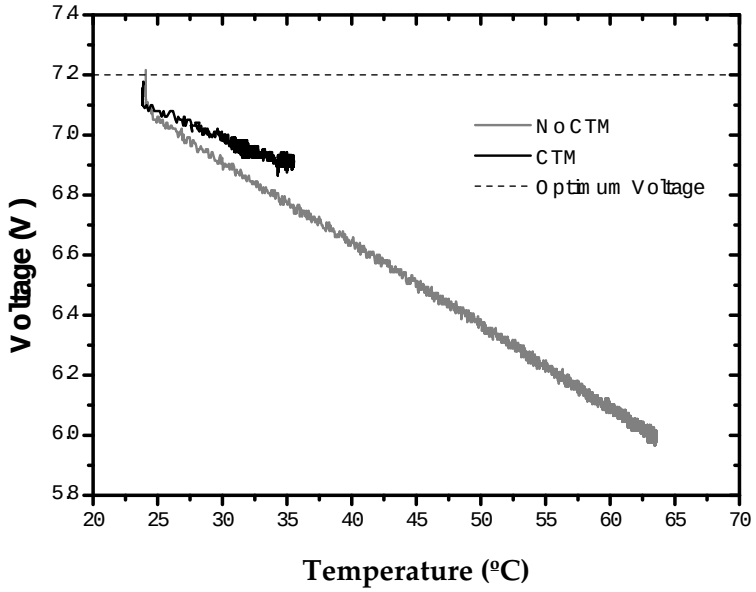

Figure 4.3: Voltage - Temperature with and without CTM

to the temperature coefficient $\Delta V/\Delta T$ and the ideal system is the one where this ratio approaches zero, meaning that the voltage supplied by the panel is not significantly influenced by its temperature. In the situation without thermal management,

$$\frac{\Delta V}{\Delta T} = 32.36\, mV\,^{\circ}C^{-1}$$

and introducing the cooling system based on constructal theory, the ratio becomes

$$\frac{\Delta V}{\Delta T} = 27.03\, mV\,^{\circ}C^{-1}$$

. It is suggested that this result reflects the effect of uniformization on the temperature distribution in the PV cell surface. Moreover, this difference of -16.5% leads to

an increase of the peak power supplied by the PV cell from $2.27\,W$ to $3\,W$. In terms of efficiency, this represents an increase of 32.3%, which is significant and shows the advantage of using water-based thermal management in PV cells, considering, for example, air-based active cooling systems that achieve increases of 12-14% (Teo *et al.* , 2012).

5 Conclusions

Thermal management plays a crucial role when improving PV cell performance. The opportunity to conceive a system that keeps its efficiency in all its life time means, to PV technology, a serious improvement to available systems in a growing market. The search for renewable sources of energy and the evermore efficient systems leads to an optimization, to improve the system overall efficiency. Adding to this, these systems provide a chance of recovering heat, fueling domestic hot water circuits, further increasing overall efficiency of the system. Meanwhile the focus is still to reduce temperature effect on PV cells and optimize their output. Therefore, the development of a very capable thermal management system is of the utmost necessity. Exploring constructal law to achieve an optimal design to the flow circuit helps accelerating the rate at which the less imperfect thermal management system is to be developed. The importance of constructal technology has not yet made its way to common engineering, but it shows a promising and powerful tool in the design of future flow networks.

In order to explore the technological potential of constructal design, an experimental facility has been developed, with which we can vary the intensity of energy incident on the PV cell and study the effect of temperature on voltage output. The design tested is based on tree-network structures that flow the coolant from a point to an area. The application of the thermal management system shows an improvement of PV cell efficiency. The tests performed took $4000\,s$, and the CTM system is capable of cooling the PV cell to temperatures $56\,\%$ below the ones obtained without cooling, thus, increasing its efficiency by $32\,\%$.

This improvement, however, does not take into consideration the parasitic energy required to feed the CTM system. Considering this, the CTM is more of a proof of concept of the application of constructal law to cooling PV cells. From this work we can suggest several guidelines for future research. Namely, the optimization of rectangular channels accordingly to the constructal law can further improve or be of assistance in future designs involving rectangular channels such as the ones conceived

in this work. This method can be reconfigured to a PV module, to exploit in full scale the viability of such a system, in terms of improved efficiency, parasitic energy and heat recovery. Following the constructal law, several geometries could also be conceived and projected into a model, such as Y-shaped bifurcations.

Bibliography

Armstrong, S., & Hurley, W. G. 2010. A thermal model for photovoltaic panels under varying atmospheric conditions. *Applied Thermal Engineering*, **30**(11-12), 1488–1495.

Bejan, Adrian, & Lorente, Sylvie. 2008. *Design with Constructal Theory.*

Bejan, Adrian, & Zane, J. Peder. 2012. *Design In Nature.*

Biwole, Pascal Henry, Eclache, Pierre, & Kuznik, Frederic. 2013. Phase-change materials to improve solar panel's performance. *Energy and Buildings*, **62**, 59–67.

Churchill, Stuart W., & Chu, Humbert H.S. 1975. Correlating equations for laminar and turbulent free convection from a horizontal cylinder. *International Journal of Heat and Mass Transfer*, **18**(9), 1049 – 1053.

Cuce, E., Bali, T., & Sekucoglu, S. a. 2011. Effects of passive cooling on performance of silicon photovoltaic cells. *International Journal of Low-Carbon Technologies*, **6**(4), 299–308.

Green, Martin a., Emery, Keith, Hishikawa, Yoshihiro, & Warta, Wilhelm. 2010. Solar cell efficiency tables (version 35). *Progress in Photovoltaics: Research and Applications*, **18**(2), 144–150.

King, D L, Boyson, W E, & Kratochvill, J a. 2004. Photovoltaic Array Performance Model. 1–43.

Luque, Antonio, & Hegedus, Steven. 2003. *Handbook of Photovoltaic Science and Engineering.* John Wiley & Sons Ltd.

Mah, Olivia. 1998. Fundamentals of Photovoltaic Materials. *National Solar Power research institute,Inc*, 1–10.

Moharram, K. a., Abd-Elhady, M. S., Kandil, H. a., & El-Sherif, H. 2013. Enhancing the performance of photovoltaic panels by water cooling. *Ain Shams Engineering Journal*, **4**(4), 869–877.

Odeh, Saad, & Behnia, Masud. 2009. Improving Photovoltaic Module Efficiency Using Water Cooling. *Heat Transfer Engineering*, **30**(6), 499–505.

Teo, H. G., Lee, P. S., & Hawlader, M. N a. 2012. An active cooling system for photovoltaic modules. *Applied Energy*, **90**(1), 309–315.

Van Helden, W. G J, Van Zolingen, R. J Ch, & Zondag, Herbert a. 2004. PV Thermal systems: PV panels supplying renewable electricity and heat. *Progress in Photovoltaics: Research and Applications*, **12**(6), 415–426.